

Evaluation of Plant Configurations for Geothermal Trigeneration Systems with Organic Rankine Cycles

Christopher Schiffler^{1*}, Florian Kaufmann¹, Ludwig Irrgang¹, Lara Kuhnert¹, Fabian Dawo¹, Christoph Wieland^{1,2}, Hartmut Spliethoff^{1,3}

¹ Technical University of Munich, Chair of Energy Systems, Garching, Germany

² Technical University of Munich, Munich School of Engineering, Garching, Bavaria, Germany

³ Bavarian Center for Applied Energy Research, Garching, Germany

*Corresponding Author: c.schiffler@tum.de

ABSTRACT

Due to the expected increasing importance of cooling applications within the next decades, geothermal trigeneration systems might be of high interest in the future. This work aims at evaluating different plant layouts against the background of more advanced plant configurations and part load behavior. Four different plant configurations are analyzed for a geothermal heat source with a temperature of 130 °C and a mass flow rate of 140 kg/s. The highest net power output is achieved by an advanced serial-parallel configuration. With an annual net power production of 25.91 GWh, the power output is between 2 and 42 % higher compared with the other three configurations (parallel, serial and serial-parallel). The application of a recuperator within the ORC system has a significant impact on the serial concepts, but only marginally increases the power output of the parallel layouts. Depending on the plant configuration, there is an optimal desorber temperature of the absorption chiller. In case of serial concepts, the desorber temperature affects only the brine reinjection temperature, but not the ORC net power. For serial concepts, an optimal desorber temperature between 65 and 70 °C is revealed. Finally, the results highlight the importance of considering part load effects when evaluating the annual performance of geothermal trigeneration systems.

1 INTRODUCTION

Deep geothermal energy is currently utilized in various countries for combined heat and power generation (CHP). For geothermal heat source temperatures below 180 °C, the application of an Organic Rankine Cycle (ORC) is the most common power generation concept (Eyerer *et al.*, 2020a). Thus, while the potential contribution of geothermal energy for the decarbonisation of the electricity and heating sector is proven by many existing projects, its possible function for a sustainable cooling supply has hardly been researched. Due to the heat island effect and the higher requirements about thermal wellbeing, the cooling demand is expected to significantly increase within the future. In contrast to electricity intensive vapor compression cycles, absorption chillers driven by geothermal energy are a promising environmental friendly alternative for cooling applications (Wang *et al.*, 2013). Therefore, geothermal trigeneration systems that can provide cooling, heating and power generation will be of high interest in the future (Lee *et al.*, 2019).

Several authors have investigated and compared potential plant layouts for geothermal trigeneration applications. Zare (2016) investigates two systems and compares an ORC system with a Kalina cycle. He then optimizes the systems regarding their exergy efficiency and examines different ORC working fluids. The systems consists of a serial connection with the power generation unit on the first level, the absorption chiller on the second level and the heat extraction on the last level. At a thermal water temperature of 120 °C, the ORC-based circuit has the higher process efficiency, while at temperatures higher than 120 °C the Kalina system achieves higher efficiencies. Pastor-Martinez *et al.* (2018) evaluate eight different plant layouts, by varying the position of an ORC system, an absorption chiller, and a heat exchanger for heating purposes. They investigate both a pure series or parallel connection as well as various combinations of the three units regarding exergy and system efficiency. The series

connection with the ORC unit at the highest temperature level followed by an absorption chiller and heat exchanger at a thermal water temperature of 150 °C leads to the highest thermal efficiency.

While the presented studies on geothermal trigeneration systems already provide some first valuable insights on the potentially favorable plant configurations, they also reveal some remaining limitations, as it is discussed in the critical review by Lee *et al.* (2019). The existing studies focus on maximizing the total energy output. Hence, the provided heating and cooling of the different configurations varies. However, it is more realistic that a geothermal trigeneration system aims at maximizing the electrical net power output while supplying the current heating and cooling demand. In addition, the fluctuating cooling and heating demand throughout one year and the resulting part load operation of the ORC system are neglected. Finally, the existing studies consider rather simple ORC configurations, meaning that the preheating, evaporating and superheating takes place within one heat exchanger. However, current research on optimized geothermal CHP configuration (e.g. by van Erdeweghe *et al.* (2017) or Eyerer *et al.* (2020b)) highlight the strong potential of advanced plant layouts that split the geothermal brine flow between the evaporator and preheater of the ORC. This approach might also be promising to increase the electrical net power output of geothermal trigeneration systems.

This work aims at evaluating different plant layouts against the background of more advanced plant configurations and part load behavior. It will provide a valuable contribution towards the further development of efficient and flexible deep geothermal trigeneration systems.

2 SYSTEM MODELLING

2.1 Demand Profiles

As pointed out by Lee *et al.* (2019), the varying heating and cooling demand over a year is neglected in most of the existing studies on geothermal trigeneration systems. Therefore, it is crucial to provide a realistic estimation of the demand characteristic. A promising approach is the VDI 4655 guideline (VDI, 2008). The idea of the guideline is to define ten typical days, which occur with a certain frequency throughout the year depending on the geographical location or climate zone. For example, the recent work by Akbari Kordlar *et al.* (2020) about a potential geothermal trigeneration system based on an advanced ammonia-water mixture cycle follows this approach. Further details can be found within the VDI 4655 guidelines and in the work by Eller *et al.* (2019).

The assumed peak heat demand of the district heating network is 20 MW_{th}, which represents the average heating capacity of geothermal CHP projects in Germany (Eyerer *et al.*, 2020a). For the district cooling network, it is assumed that one industrial consumer (e.g. a data center) has a constant base load demand of 2 MW. In addition, for higher ambient temperatures, an additional cooling demand for room cooling arises. Thus, the cooling demand increases up to 6.2 MW during summer days. Table 1 summarizes the demand profiles as well as the ambient temperature of the ten different day types. Furthermore, next to the overall heating and cooling demand, the required supply and return temperatures of the district heating and cooling network need to be defined. A supply temperature of 90 °C and a return temperature of 60 °C is assumed for the district heating network, which represents the common third generation of district heating networks (Lund *et al.*, 2014). For the district cooling network, a return temperature of 12 °C and a supply temperature of 6 °C is considered.

Table 1: Assumed daily mean values of the ambient temperature, heating demand and cooling demand for the ten different day categories.

Day category ¹	WWF	WWC	WSF	WSC	TWC	TSC	TSF	TWF	SWX	SSX
Number of days	n=29	n=91	n=6	n=19	n=72	n=10	n=15	n=37	n=13	n=73
$T_{ambient}$ [°C]	-0.13	-5.68	2.27	1.10	7.37	4.81	13.8	15.4	15.67	17.24
$\dot{Q}_{heating}$ [MW]	19.8	19.7	20	18.3	10.7	10.4	8.0	9.6	5.1	4.9
$\dot{Q}_{cooling}$ [MW]	2	2	2	2	2	2	5.0	5.2	6.1	6.2

¹ The first letter of the category is either “S” for summer, “W” for winter or “T” for the transitional period. The second letter is either “W” for workdays (including Saturdays) or “S” for Sundays. The third letter accounts for the cloudiness and is “B” for bright days or “C” for cloudy days. For summer days, the cloudiness has little impact on the daily temperature curve, so it is neglected, and the third letter is simply “X”.

2.2 Plant Configurations

As already discussed in Section 1, there is a high variety of potential plant configurations for geothermal trigeneration systems. This work compares an advanced plant layout with three already proposed systems. Figure 1 visualizes the plant configurations of the four considered concepts. Firstly, a serial concept (SC) is investigated, following the layout presented by Zare (2016). In this case, the geothermal brine first flows through the ORC system, before passing through the desorber of the absorption chiller and the heat exchanger for the district heating system. In this concept, the brine outlet temperature of the ORC is determined by the fact that the brine temperature before the district heating supply needs to be above the required supply temperature of the district heating network. Secondly, a parallel concept (PC) is considered, which was investigated (among other concepts) by Pastor-Martinez *et al.* (2018). Here, the brine is separated into three different streams. The available brine mass flow rate for the ORC is determined by the required flow rates of the other two streams necessary to supply the current heating and cooling demand. The third option is a serial-parallel concept (SPC). After the brine has passed through the ORC, the brine flow is separated into two streams for both the cooling and heating application (Pastor-Martinez *et al.*, 2018). Similar to the PC concept, the minimal possible brine temperature after the ORC preheater is specified by the required brine temperature for the district heating supply. Finally, an advanced serial parallel concept (ASPC) is investigated. In this case, the brine flow is divided after the evaporator. The complete brine flow is available for the evaporation and superheating of the ORC system. In addition, the brine temperature after the ORC preheater is not limited by the required temperature of the cooling and heating application. Finally, for days with high heating demand, the option of a small bypass flow is considered. Depending on the chosen evaporation pressure of the ORC system (and thus affecting the brine outlet temperature of the evaporator) the bypass might be necessary to provide the required temperature level for the heating and cooling supply. A parameter optimization is carried out in order to find the optimal system parameter for each day type. Depending on the plant layout an internal recuperator might have a positive effect of the system performance. Within the result section, the effect of an internal recuperator for the four different investigated plant layouts will be evaluated. However, for the sake of clarity, the internal recuperator is not visualized within Figure 1.

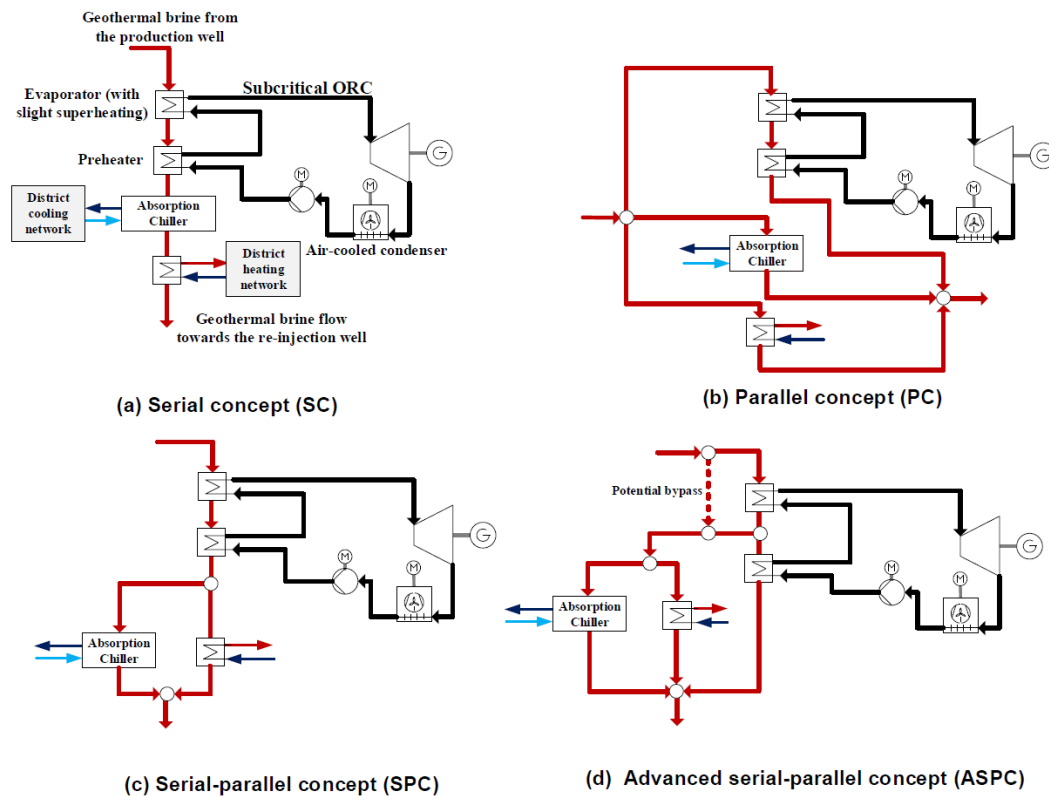


Figure 1: Plant layout of the different investigated concepts

2.3 Modelling of the Absorption Chiller

Depending on the required temperature level of cooling, either lithium bromide – water or water – ammonia mixtures are applied within the absorption chiller (Pastor-Martinez *et al.*, 2018). In this work, a standard lithium bromide – water absorption chiller is considered, providing cooling at 5 °C while having absorber and condenser temperatures of 40 °C. Therefore, the assumed absorption chiller could supply a potential district cooling systems, which normally have a supply temperature between 6 and 8 °C. A detailed MATLAB simulation model is developed, following the methodology presented by Wonchala *et al.* (2014). The thermodynamic property data of the lithium bromide – water mixture are derived from Pátek and Klomfar (2006). The performance of the absorption chiller is characterized by the Coefficient of Performance (COP), which describes the ratio between the desired output (cooling by the evaporator) and the necessary input (heat input by the geothermal brine to the desorber and the pump power):

$$COP = \frac{\dot{Q}_{evap}}{\dot{Q}_{des} + \dot{W}_{pump}}$$

In comparison to vapor compression cycles, absorption chillers only require a marginal electricity demand. Even for the day type SSX with the highest cooling demand of 6.2 MW, the required electrical pump power of the modelled absorption chiller is below 15 kW. Even if we assume real power consumption to be significantly higher, in comparison to the power output by the ORC within a range of a few MW, the required pump power of the absorption chiller is negligible.

Figure 2 visualizes both the layout of the absorption chiller as well as the relation between the COP and the desorber temperature. The figure reveals that the COP is mainly constant for desorber temperatures above 75 °C. For lower desorber temperatures, the COP starts to decrease significantly. For example, in case of a desorber temperature below 60 °C, the COP is only around 0.2. This highlights that the choice of the operation temperature of the absorption chiller might have some significant impact on the operational performance of the trigeneration system. While a lower desorber temperature reduces the COP (and therefore increases the required heat demand to provide the same amount of cooling), more heat on a higher temperature level is available for the ORC system, which might therefore increase the power output of the ORC. In order to evaluate this potential trade-off, a detailed evaluation of the optimal desorber temperature for the different plant configurations will be presented within the result section.

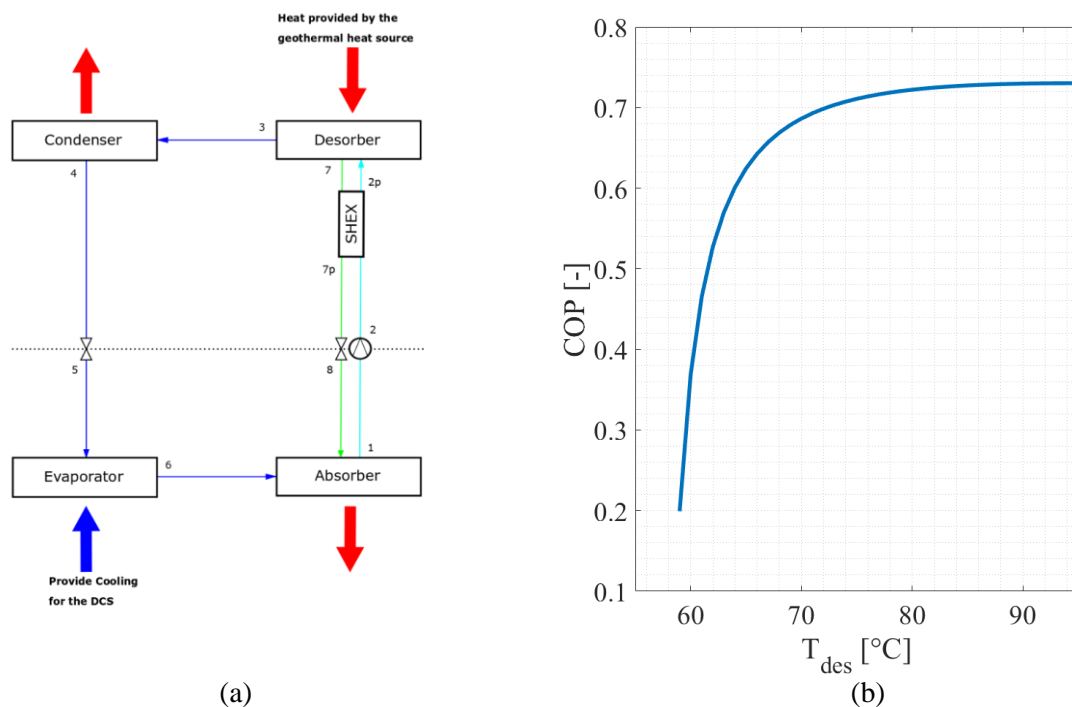


Figure 2: Visualization of the (a) absorption chiller layout and (b) the relation of the COP and the desorber temperature.

2.4 Modelling of the ORC

This work considers a geothermal heat source with a temperature of 130 °C and a mass flow rate of 140 kg/s. Both values represent realistic parameters of existing deep geothermal CHP projects within the South German Molasse Basin, which is currently the most active region for geothermal projects in Germany (Eyerer et al., 2020a). R1233zd(E) is considered as the ORC working fluid, since it is a promising environmentally friendly alternative for the common high-GWP working fluid R245fa as shown by the Life Cycle Assessments of Heberle et al. (2016) and Dawo et al. (2021). The simulation of the ORC system is carried out by the commercial process simulation software Epsilon Professional 14. A superheating of 3 K and a minimal required pinch point of 3 K for each heat exchanger is assumed. Pressure drops within the heat exchangers are neglected. Table 2 summarizes the main model parameters. More information about the justification of the different model parameters can be found in a previous work of the authors (Schifflechner et al., 2020). The required electrical power of the brine pump is not considered, since the actual power demand depends strongly on the actual local geological conditions of a geothermal project (Eyerer et al., 2020a). The part load behavior of the ORC turbine is modelled based on the part load model developed by (Dawo et al., 2019). The model describes the change of the isentropic turbine coefficient by considering potential deviations of the ORC mass flow rate and turbine outlet pressure from the operational point with the maximal power (MP) output. For each plant configuration and day type, the optimal evaporation pressure was determined by an optimization routine.

$$\eta_{is,T,PL} = \eta_{is,T,MP} \left[a_{00} + a_{10} \cdot \left(\frac{\dot{m}}{\dot{m}_{MP}} \right) + a_{01} \cdot \left(\frac{p}{p_{MP}} \right) + a_{20} \cdot \left(\frac{\dot{m}}{\dot{m}_{MP}} \right)^2 + a_{11} \cdot \left(\frac{\dot{m}}{\dot{m}_{MP}} \right) \cdot \left(\frac{p}{p_{MP}} \right) \right]$$

with: $a_{00} = -0.0429$; $a_{10} = 1.781$; $a_{01} = 0.2781$; $a_{20} = -0.5579$; $a_{11} = -0.4609$.

The part-load behaviour of the heat exchanger is modelled by following the methodology described by Manente *et al.* (2013) and Dawo *et al.* (2019). However, since this work does not consider an economic evaluation and optimization (based on the required heat transfer area of the different heat exchangers), the part-load behaviour of the heat exchangers has a negligible effect on the results of the work, since the ORC on-design point is set for the day type with the highest ORC power output, which is also the day type with the highest amount of heat transfer from the geothermal brine to the ORC.

Table 2: Main model parameters.

Parameter	Value
T_{WH}	130 °C
\dot{m}_{WH}	140 kg/s
$p_{evap,ORC}$	Optimized for each configuration and day type ²
$T_{ORC,superheating}$	3 K
$\eta_{is,T,MP}$	0.8
$\eta_{is,Pump}$	0.8
$\eta_{generator}$	0.98
COP of the Absorption Chiller	0.71 ³
Minimal required Pinch Point temperature of each heat exchanger	3 K
Electricity demand of the air cooled condenser	0.15 kW per kg s ⁻¹ of air flow

² The evaporation pressure is varied in 0.25 bar steps for each type day and plant configuration, in order to determine the optimal evaporation pressure that results in the highest ORC net power output.

³ The base scenario considers a desorber temperature of 75 °C.

3 RESULTS AND DISCUSSION

Table 3 summarizes the results of the ORC systems' electrical net power and the brine reinjection temperature for the different day types and evaluated plant configurations. The results reveal that the ASPC configuration provides the highest net power output of the ORC system over the year. With an annual net power production of 25.91 GWh, the power output is between 2 and 42 % higher compared with the other three configurations. The lowest electricity amount is achieved by the PC configuration (17.88 GWh), while the SC layout results in 21.99 GWh. It is noteworthy that the annual electricity production of the SPC is only 2 % lower than by the ASPC layout, even though the maximum net power performance of the ASPC configuration on the day type *TSC* is around 700 kW higher compared with the SPC layout. However, the ASPC configuration leads to a significantly lower power output during the winter days. This effect is caused by the different part load behavior of both configurations. The SPC configuration displays only marginal part load behavior, since the available brine mass flow rate is constant during the year. However, in case of the ASPC configuration, the available brine flow rate deviates. Therefore, the consideration of the resulting part load operation reduces the achievable net power output by more than 600 kW compared with a model neglecting part load effects. Hence, the results highlight the importance of considering part load effects when evaluating the annual performance of geothermal trigeneration systems.

Depending on the system concept, there are considerable variations of the reinjection temperatures. The highest average annual reinjection temperature of 80.4 °C occurs with the SC concept. For the other three concepts, they are 62.2 °C (PC), 62.1 °C (SPC) and 52.2 °C (ASPC) respectively.

Table 3: Summary of the results for the different day types.

Day type	SC		PC		SPC		ASPC	
	$P_{el,net}$ [MW]	T_{reinj} [°C]						
WWF	2.86	58.2	1.80	58.6	3.16	53.5	2.72	52.6
WWC	3.07	57.9	2.02	57.7	3.32	53.5	2.98	54.2
WSF	2.81	57.9	1.69	56.4	3.05	53.1	2.46	52.5
WSC	2.85	60.8	1.91	56.4	3.10	56.1	2.79	56.4
TWC	2.64	74.4	2.70	56.4	2.88	69.0	3.56	53.4
TSC	2.72	74.3	2.73	63.7	3.04	69.5	3.75	53.3
TSF	1.99	78.5	1.99	65.4	2.63	66.6	2.83	56.4
TWF	1.95	75.9	1.75	65.1	2.57	63.2	2.58	56.2
SWX	1.94	83.1	1.96	68.4	2.56	68.9	2.78	57.8
SSX	1.90	83.1	1.85	68.1	2.50	69.0	2.66	58.3
Annual net electricity production	21.99 GWh		17.88 GWh		25.40 GWh		25.91 GWh	

Figure 3 visualizes the effect of the absorption chiller's generator temperature on the achievable ORC net power output. As discussed in Section 2.3, there is an expected optimal generator temperature for some of the plant configurations. Since a lower desorber temperature reduces the COP (and therefore increases the required heat demand to provide the same amount of cooling), more heat on a higher temperature level is available for the ORC system. The choice of the desorber temperature has no effect on the SPC layout, since the ORC outlet temperature is already defined by the required temperature level of the district heating system. Hence, the desorber temperature would only affect the brine reinjection temperature. However, as shown by the results in Figure 3, the generator temperature can have a significant impact on the achievable ORC net power for the PC and ASPC configuration. Both (semi) parallel configurations reveal an optimal desorber temperature of the absorption chiller between 65 and 70 °C. This demonstrates the importance of the optimal selection of the absorption chiller's operational conditions in case of parallel trigeneration configurations. It needs to be considered that these results are obtained for a standard LiBr-H₂O absorption chiller. However, in case of further more complex absorption chiller types (e.g. double lift or double effect cycles) the optimal desorber temperature might differ.

Furthermore, the impact of a recuperator was investigated. Table 4 summarizes the results for the day type *TSC*. The effect of the recuperator depends on the general concept of the plant layout. In case of the both serial layouts (SC and SPC), the recuperator increases the achievable net power by up to 7 %. The recuperator increases the ORC efficiency (and therefore the net power output), but has no impact of the brine reinjection temperature, since this temperature is determined by the heating and cooling demand. The recuperator has only a marginal positive effect (< 1 %) for both parallel layouts (PC and ASPC). Within this work, a recuperator is also considered for the parallel layouts, but in case of an actual geothermal project, the recuperator might be neglected in order to minimize the investment costs.

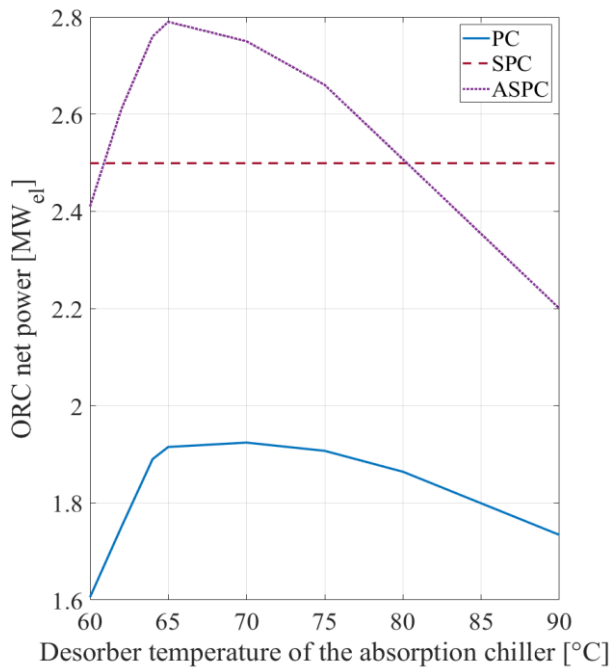


Figure 3: Effect of the generator temperature of the absorption chiller on the ORC net power output for the day type *SSX*⁴.

Table 4: Effect of the recuperator on the electrical power output and reinjection temperature for the day type *TSC*.

	With recuperator		Without recuperator	
	$P_{el,net}$ [MW]	T_{reinj} [°C]	$P_{el,net}$ [MW]	T_{reinj} [°C]
SC	2.72	74.3	2.57	74.3
PC	2.73	63.7	2.70	61.2
SPC	3.04	69.5	2.85	69.5
ASPC	3.75	53.3	3.71	49.9

4 CONCLUSIONS AND OUTLOOK

Due to the expected increasing importance of cooling applications within the next decades, geothermal trigeneration systems might be of high interest in the future. This paper investigates several potential plant configurations especially against the background of the varying heating and cooling demand within one year and the resulting part load behavior. In this paper, four different plant configurations are analyzed for a geothermal heat source with a temperature of 130 °C and a mass flow rate of 140 kg/s. The summarized key findings are:

- The ASPC configuration provides the highest net power output of the ORC system over the year. With an annual net power production of 25.91 GWh, the power output is between 2 and 42 % higher compared with the other three configurations.
- The annual electricity production of the SPC is only 2 % lower than by the ASPC layout, even though the maximum net power performance of the ASPC configuration on the day type *TSC* is around 700 kW higher compared with the SPC layout. However, the ASPC configuration leads to a significantly lower power output during the winter days due to its strong part load

⁴ No graph is shown for the sole serial configuration (SC), since in this case the desorber temperature is predetermined by the required temperature level after the absorption chiller in order to provide the necessary supply temperature of the district heating network.

characteristic. Hence, the results highlight the importance of considering part load effects when evaluating the annual performance of geothermal trigeneration systems.

- The application of a recuperator within the ORC system has a significant impact on the serial concepts SC and SPC, but only marginally increases the power output of the PC and ASPC layout.
- Depending on the plant configuration, there is an optimal desorber temperature of the absorption chiller. In case of the SC and SPC layout, the desorber temperature affects only the brine reinjection temperature, but not the ORC net power. For both the PC and ASPC concept, an optimal desorber temperature between 65 and 70 °C is revealed.

Thus, while this work provides some first valuable insights on the achievable performance increases of geothermal trigeneration systems by more advanced plant configurations, there are still several aspects, which might be considered in future studies. Firstly, more advanced plant layouts, such as considering a regenerative ORC concept presented by Eyerer *et al.* (2020b), might further improve the plant performance. The same applies for more advanced absorption chiller configurations (cf. Xu and Wang (2016)). Secondly, different geothermal heat source temperatures and application scenarios (e.g. different generation of district heating networks) should be evaluated. Finally, a techno-economic evaluation would provide valuable insights about the expected economic performance of different plant configurations and application scenarios.

NOMENCLATURE

Symbols

COP	Coefficient of Performance	(-)
\dot{m}	Mass flow	(kg/s)
p	Pressure	(kPa)
P	Power	(W)
\dot{Q}	Heat flow	(W)
T	Temperature	(K)
η	Efficiency	(-)

Abbreviations

ASPC	Advanced Serial-Parallel Concept
CHP	Combined heat and power generation
ORC	Organic Rankine Cycle
PC	Parallel Concept
SC	Serial Concept
SPC	Serial-Parallel Concept

Subscripts

amb	Ambient
des	Desorber
evap	Evaporation
el	Electrical
is	Isentropic
MP	Maximal Power
PL	Part Load
T	Turbine
WH	Wellhead

REFERENCES

- Akbari Kordlar, M., F. Heberle, and D. Brüggemann, 2020, "Evaluation and Optimization of the Annual Performance of a Novel Tri-Generation System Driven by Geothermal Brine in Off-Design Conditions," *Applied Sciences* **10**, 6532.
- Dawo, F., J. Fleischmann, F. Kaufmann, C. Schiffler, S. Eyerer, C. Wieland, and H. Spliethoff, 2021, "R1224yd(Z), R1233zd(E) and R1336mzz(Z) as replacements for R245fa: Experimental performance, interaction with lubricants and environmental impact," *Applied Energy* **288**, 116661.

- Dawo, F., C. Wieland, and H. Spliethoff, 2019, “Kalina power plant part load modeling: Comparison of different approaches to model part load behavior and validation on real operating data,” *Energy* **174**, 625.
- Eyerer, S., C. Schiffelechner, S. Hofbauer, W. Bauer, C. Wieland, and H. Spliethoff, 2020a, “Combined heat and power from hydrothermal geothermal resources in Germany: An assessment of the potential,” *Renewable and Sustainable Energy Reviews* **120**, 109661.
- Eyerer, S., F. Dawo, C. Wieland, and H. Spliethoff, 2020b, “Advanced ORC architecture for geothermal combined heat and power generation,” *Energy* **205**, 117967.
- Heberle, F., C. Schiffelechner, and D. Brüggemann, 2016, “Life cycle assessment of Organic Rankine Cycles for geothermal power generation considering low-GWP working fluids,” *Geothermics* **64**, 392.
- Lee, I., J. W. Tester, and F. You, 2019, “Systems analysis, design, and optimization of geothermal energy systems for power production and polygeneration: State-of-the-art and future challenges,” *Renewable and Sustainable Energy Reviews* **109**, 551.
- Lund, H., S. Werner, R. Wiltshire, S. Svendsen, J. E. Thorsen, F. Hvelplund, and B. V. Mathiesen, 2014, “4th Generation District Heating (4GDH): Integrating smart thermal grids into future sustainable energy systems,” *Energy* **68**, 1
- Manente, G., A. Toffolo, A. Lazzaretto, and M. Paci, 2013, “An Organic Rankine Cycle off-design model for the search of the optimal control strategy,” *Energy* **58**, 97.
- Pastor-Martinez, E., C. Rubio-Maya, V. M. Ambriz-Díaz, J. M. Belman-Flores, and J. J. Pacheco-Ibarra, 2018, “Energetic and exergetic performance comparison of different polygeneration arrangements utilizing geothermal energy in cascade,” *Energy Conversion and Management* **168**, 252.
- Pátek, J., and J. Klomfar, 2006, “A computationally effective formulation of the thermodynamic properties of LiBr–H₂O solutions from 273 to 500K over full composition range,” *International Journal of Refrigeration* **29**, 566.
- Schiffelechner, C., F. Dawo, S. Eyerer, C. Wieland, and H. Spliethoff, 2020, “Thermodynamic comparison of direct supercritical CO₂ and indirect brine-ORC concepts for geothermal combined heat and power generation,” *Renewable Energy* **161**, 1292.
<https://doi.org/10.1016/j.renene.2020.07.044>
- van Erdeweghe, S., J. van Bael, B. Laenen, and W. D’haeseleer, 2017, ““Preheat-parallel” configuration for low-temperature geothermally-fed CHP plants,” *Energy Conversion and Management* **142**, 117.
- VDI-Gesellschaft Energietechnik, 2008, *Referenzlastprofile von Ein- und REferenzlastprofile von Ein- und Mehrfamilienhäusern für den Einsatz von KWK-Anlagen*.
- Wang, X., A. Bierwirth, A. Christ, P. Whittaker, K. Regenauer-Lieb, and H. T. Chua, 2013, “Application of geothermal absorption air-conditioning system: A case study,” *Applied Thermal Engineering* **50**, 71.
- Wonchala, J., M. Hazledine, and K. Goni Boulama, 2014, “Solution procedure and performance evaluation for a water–LiBr absorption refrigeration machine,” *Energy* **65**, 272.
- Xu, Z. Y., and R. Z. Wang, 2016, “Absorption refrigeration cycles: Categorized based on the cycle construction,” *International Journal of Refrigeration* **62**, 114.
- Zare, V., 2016, “A comparative thermodynamic analysis of two tri-generation systems utilizing low-grade geothermal energy,” *Energy Conversion and Management* **118**, 264.

ACKNOWLEDGEMENT

Funding from the Bavarian State Ministry of Education, Science and the Arts in the framework of the project Geothermal-Alliance Bavaria is gratefully acknowledged.